50272-101

| REPORT DOCUMENTATION PAGE | 1. REPORT NO. NSF/RA -770631 | 2. | 3. Recipient's Accession No. PB285987 |
|---|---|---|---|
| 4. Title and Subtitle: Underground Pipe Damages and Ground Characteristics, Technical Report No. CU-1 | | | 5. Report Date: June 1977<br>6. |
| 7. Author(s): M. Shinozuka, H. Kawakami | | | 8. Performing Organization Rept. No. CU-1 |
| 9. Performing Organization Name and Address: Columbia University<br>Department of Civil Engineering and Engineering Mechanics<br>New York, New York 10027 | | | 10. Project/Task/Work Unit No.<br>11. Contract(C) or Grant(G) No.<br>(C) ENV7609838<br>(G) |
| 12. Sponsoring Organization Name and Address: Applied Science and Research Applications (ASRA)<br>National Science Foundation<br>1800 G Street, N.W.<br>Washington, D.C. 20550 | | | 13. Type of Report & Period Covered: Technical<br>14. |

15. Supplementary Notes

16. Abstract (Limit: 200 words)

A method is proposed under the quasi-two-dimensional free field conditions to evaluate the elastic surface strains arising from spatial variability of the soil property (ground predominant frequency) of a surface layer subjected to shear waves incident vertically from below through a semi-infinite firm ground. The variability is described in terms of a random function of the space variable characterized by mean value, variance and correlation distance. Applying the method, the strains are evaluated for the metropolitan Tokyo area on the basis of the local soil conditions, and a reasonable correlation has been established between such strains and the damage statistics collected on the underground water supply pipeline under the 1923 Kanto Earthquake. This investigation is currently being extended so that the free field strains are evaluated not at the free ground surface but at a usual depth for underground water supply pipelines.

17. Document Analysis a. Descriptors

Seismic waves
Soil dynamics
Earthquakes
Water pipelines
Interfacial tension
Wave propagation
Elastic properties

b. Identifiers/Open-Ended Terms

Elastic surface strains
Earthquake-induced damage statistics
Underground water supply pipelines
Tokyo

c. COSATI Field/Group

| 18. Availability Statement | 19. Security Class (This Report) | 21. No. of Pages |
|---|---|---|
| NTIS. | | 17 |
| | 20. Security Class (This Page) | 22. Price MFA01 PC A02 |

(See ANSI-Z39.18) See Instructions on Reverse

OPTIONAL FORM 272 (4-77)
(Formerly NTIS-35)
Department of Commerce

This paper is presented at the Lifeline Earthquake Engineering Specialty Conference at the University of California, Los Angeles, August 30-31, 1977

# UNDERGROUND PIPE DAMAGES AND GROUND CHARACTERISTICS

by

Masanobu Shinozuka* and Hideji Kawakami**

ABSTRACT

A method is proposed under the quasi-two-dimensional free field conditions to evaluate the elastic surface strains arising from spatial variability of the soil property (ground predominant frequency) of a surface layer subjected to shear waves incident vertically from below through a semi-infinite firm ground. The variability is described in terms of a random function of the space variable characterized by mean value, variance and correlation distance. Applying the method, the strains are evaluated for the metropolitan Tokyo area on the basis of the local soil conditions, and a reasonable correlation has been established between such strains and the damage statistics collected on the underground water supply pipelines under the 1923 Kanto Earthquake.

## 1. MODEL FOR GROUND AND INCIDENT WAVES

A surface layer of depth H resting on a semi-infinite firm ground as shown in Fig. 1 is considered. A plane shear wave $u_o$ with the only non-zero displacement component u in the x direction is incident vertically to the surface layer from below.

$$u_o = A_o \exp\{i(\omega t - k_2 z)\} \tag{1}$$

Using subscripts 1 and 2 respectively for the quantities of the surface layer and of the firm ground, we have the following differential equation for the displacements under the shear beam assumption;

$$\rho_i \frac{\partial^2 u_i}{\partial t^2} = \mu_i \frac{\partial^2 u_i}{\partial z^2} \qquad (i = 1,2) \tag{2}$$

subject to the boundary conditions.

$$u_1 = u_2 \quad \text{and} \quad \mu_1 \partial u_1/\partial z = \mu_2 \partial u_2/\partial z \quad \text{at } z = 0 \tag{3}$$

and

$$\partial u_1/\partial z = 0 \qquad \text{at} \quad z = H \tag{4}$$

where $\rho$ = mass density and $\mu$ = shear rigidity of the medium. The

*Professor of Civil Engineering, Member, ASCE, Columbia University, New York, N. Y.

**Senior Research Assistant, Department of Civil Engineering and Engineering Mechanics, Columbia University, New York, N. Y.

solution to this boundary value problem can be given in terms of combinations of incident, reflected and refracted waves as

$$u_2 = A_o \exp\{i(\omega t - k_2 z)\} + A \exp\{i(\omega t + k_2 z)\} \quad (5)$$

$$u_1 = B \exp\{i(\omega t - k_1 z)\} + C \exp\{i(\omega t + k_1 z)\} \quad (6)$$

When the incident wave is the real part of Eq. 1 or

$$u_o = A_o \cos(\omega t - k_2 z) \quad (7)$$

with $A_o$ being real, the displacement at the ground surface, $u(H,t)$, can be written as

$$u(H,t) = \frac{2A_o}{\sqrt{\cos^2 k_1 H + \alpha^2 \sin^2 k_1 H}} \cos(\omega t - \delta) \quad (8)$$

where

$$\delta = \tan^{-1} \frac{\alpha \sin k_1 H}{\cos k_1 H} \quad (9)$$

and

$$\alpha = \rho_1 V_1 / (\rho_2 V_2) \quad (10)$$

with $V_1 = \sqrt{\mu_1/\rho_1}$ and $V_2 = \sqrt{\mu_2/\rho_2}$ being the shear velocity of the surface layer and the firm ground, respectively.

If we define the amplification factor M as the ratio of the amplitude of $u(H,t)$ to that of the incident wave, then

$$M = 2/\sqrt{\cos^2 k_1 H + \alpha^2 \sin^2 k_1 H} \quad (11)$$

Using the following relationship among wave number $k_1$, depth H of the surface layer and frequency $f = \omega/(2\pi)$ of the incident wave

$$k_1 H = \omega H / V_1 = 2\pi f H / V_1 = 2\pi H / (V_1 T) \quad (12)$$

we plot in Fig. 2 the amplification factor M as a function of $H/(V_1 T)$ with $\alpha = 1/3$. Figure 2 exhibits peak values of $2/\alpha$ at $H/(V_1 T) = 1/4, 3/4, 5/4, \ldots$ and trough values of 2.0 at $H/(V_1 T) = 0, 1/2, 1, 3/2, \ldots$. Therefore, the frequency values $f = V_1/(4H), 3V_1/(4H), 5V_1/(4H)$, may be interpreted as the predominant frequencies of the ground given $V_1$ and H. When the damping and nonhomogeneity (along the depth or along the shear beam) of the soil material are taken into consideration to reflect the reality more closely, the amplification factor exhibits a rather irregular shape as a function of the frequency of the incident wave usually with identifiable peaks at two or three frequencies, higher peaks at smaller frequencies. The predominant frequency of the ground under these circumstances may be defined as the mean of such frequencies weighted on the magnitudes of the corresponding peak values.

For the purpose of the present investigation, however, we consider that the predominant frequency $f_p$ of the ground is determined by

$$f_p = V_1/(4H) \tag{13}$$

If the incident wave is of the form

$$u_o = \sqrt{2} \sum_{i=1}^{n} A_{oi} \cos(\omega_i t - k_{2i} z + \phi_i) \tag{14}$$

then, because of linearity, the displacement at the ground surface can be written as

$$u(H,t) = \sqrt{2} \sum_{i=1}^{n} \frac{2A_{oi}}{\sqrt{\cos^2 k_{1i}H + \alpha^2 \sin^2 k_{1i}H}} \cos(\omega_i t - \delta_i + \phi_i) \tag{15}$$

where

$$k_{1i}H = \omega_i H/V_1 \tag{16}$$

and

$$\delta_i = \tan^{-1} \frac{\alpha \sin k_{1i}H}{\cos k_{1i}H} \tag{17}$$

It is important to note that Eq. 14 represents, in the limit as $n \to \infty$, a stationary Gaussian random process[1] with zero mean and one-sided spectral density $S_o(\omega)$ if

$$A_{oi} = \sqrt{S_o(\omega_i)\,\Delta\omega} \tag{18}$$

and $\phi_i$ are the random phase angles independently and uniformly distributed between 0 and $2\pi$. In Eqs. 15 and 18,

$$\omega_i = i\Delta\omega \tag{19}$$

and

$$\omega_n = n\Delta\omega \tag{20}$$

is the upper cut-off frequency beyond which the spectral density is assumed to be zero.

In the present study, the incident "acceleration" wave is assumed to have the one-sided spectral density of the following form.

$$S_A(\omega) = \frac{25\,\omega^2/289}{(1-\omega^2/242)^2 + \omega^2/289} \cdot \frac{100^2}{559} \tag{21}$$

This is of the same analytical form as suggested in Ref. 2. However, the parameter values are so adjusted that the spectral density will produce the standard deviation of 100 gal. Figure 3 plots $S_A(\omega)$ in the range $\omega = 0$ to 200 rad/sec. The spectral density $S_o(\omega)$ of the displacement corresponding to Eq. 21 is obtained as $S_o(\omega) = S_A(\omega)/\omega^4$ with a truncation for the values of $\omega$ less than 0.6 rad/sec to make the standard deviation of the displacement process a finite value (in this case 2.1 cm). When the spectral density $S_o(\omega)$ is used in Eq. 15 through Eq. 18, the displacement $u(H,t)$ at the ground surface becomes a stationary Gaussian process with zero mean and the variance equal to

$$4 \sum_{i=1}^{n} S_o(\omega_i)\Delta\omega/(\cos^2 k_{1i}H + \alpha^2 \sin^2 k_{1i}H)$$

provided that $\phi_i$ are the random phase angles as defined before.

A sample function of the incident displacement wave given in Eq. 14 (with z = 0) is plotted over a stretch of 6.3 seconds in Fig. 4. For this purpose, Eqs. 14, 19 and 20 are used with $\Delta\omega$ = 0.6 rad/sec, $\omega_n$ = 76.8 rad/sec and hence n = 128.

## 2. VARIABILITY OF THE SOIL PROPERTY

Referring to Fig. 1, consider an underground pipeline horizontally placed along the x-direction and extending across a vertical interface perpendicular to the x-axis which separates the surface layer into two elastic media of different elastic constants. A recent study [3] concludes that extensive stresses and strains arise in such a pipeline at the point of interface under the type of incident wave as described in the preceding section. This indicates a possible high sensitivity of pipeline stresses and strains to the variability of the soil property along the pipe axis. Therefore, the present study primarily investigates the effect of the variability of soil property along the direction of pipe axis on the extent of earthquake-induced damages of underground pipelines. For this purpose we interpret the variability as a random function of x disregarding at this time the variability in the z direction.

To be specific, we assume that the predominant frequency $f_p$ is a random function of x; $f_p = f_p(x)$. Because of Eq. 13, this implies that the shear velocity $V_1$ of the surface layer is also a random function of x; $V_1 = V_1(x)$. As a first approximation, it is assumed that the predominant frequency is a stationary Gaussian process with

$$E[f_p(x)] = \mu_f \tag{22}$$

and

$$E[f_p(x) f_p(x + \xi)] = \overline{\sigma_f}^2 \phi(\xi) + \mu_f^2 \tag{23}$$

when $\xi$ is the separation distance between two points at which the predominant frequencies are considered, $\overline{\sigma_f}$ is the standard deviation, and $\phi(\xi)$ is the normalized autocovariance function of the process;

$$\phi(\xi) = (1 - 2|\xi/L|^2) \exp\{-|\xi/L|^2\} \tag{24}$$

The Wiener-Khintchine transform of Eq. 23 results in the one-sided spectral density G(k) of $f_p(x)$.

$$G(k) = \frac{\overline{\sigma_f}^2 L^3 k^2}{2\sqrt{\pi}} \exp\{-k^2L^2/4\} + 2\mu_f^2 \delta(k) \tag{25}$$

where $\delta(k)$ is the Dirac delta function. Equation 24 has been chosen for its simplicity, analytical tractability and possible compatibility with the reality, but mainly for the reason that the derivative of $f_p(x)$ with respect to x exists at least in the mean square sense. Other significant characteristics that can be derived from Eqs. 24 and 25 are $\omega_a$ = apparent frequency (expected rate of positive zero crossing x $2\pi$), $\nu$ = expected rate of local maxima x $2\pi$, and $\varepsilon = \omega_a/\nu$ = irregularity factor such that

$$\omega_a = \sqrt{6}/L, \quad \nu = \sqrt{10}/L \quad \text{and} \quad \varepsilon = 0.77 \tag{26}$$

The normalized autocovariance function $\phi(\xi)$ is plotted in Fig. 5 while the spectral density G(k) with L = 100 m in Fig. 6. The physical significance of L in Eqs. 24 and 25 is quite important; L has the dimension of length with a smaller value implying a shorter distance in which the correlation disappears. In the present study, the parameter L is called the "correlation distance" for convenience. If the degree of uniformity or homogeneity of the surface layer is termed "smoothness" as some researchers prefer, then the larger the correlation distance, the smoother the layer. To visualize this point, simulated sample function of $f_p(x)$ in the form

$$f_p(x) = \sqrt{2} \sum_{i=1}^{n} B_{oi} \cos(k_i x + \phi_i) \tag{27}$$

where L = 100 m and 500 m over an 1,000 m interval are respectively shown in Figs. 7(a) and 8(a) with $\mu_f = 3.0\,\text{Hz}$ and $\sigma_f^2 = 0.5\,\text{Hz}^2$. Also, note that these figures have the $V_1$ scale corresponding to the $f_p$ scale (H = 20 m). As expected, we observe a more rapid variation of $f_p$ in case of L = 100 m than in the case of L = 500 m. In Eq. 27

$$B_{oi} = \sqrt{G(k_i)\,\Delta k} \tag{28}$$

with $k_i = i\Delta k$. The cut-off wave number $k_n = n\Delta k$ has the same significance as $\omega_n$ in Eq. 20, and $\phi_i$ are the random phase angles.

Although the correlation distance L does indicate the extent of the soil property variability as seen above, it is neither a direct nor familiar measure with which the degree of earthquake-induced damage of the underground pipelines can be associated. In the present study, the intensity of the surface strain (to be defined in the following section) that strictly results from the property variability of the surface layer is used as the measure of such variability to be correlated to the damage statistics.

## 3. STRAIN DISTRIBUTION

Introducing the variability $f_p$ into Eq. 15, we can write the displacement at the ground surface as

$$u(H,t,f_p) = \sqrt{2} \sum_{i=1}^{n} 2A_{oi} q_i^{-1/2} \cos\{\omega_i t + \theta_i\} \tag{29}$$

where $A_{oi}$ is as given by Eq. 18,

$$q_i = \cos^2\left(\frac{\omega_i}{4f_p}\right) + \left(\frac{4Hf_p}{V_2}\right)^2 \sin^2\left(\frac{\omega_i}{4f_p}\right) \quad (\rho_1 = \rho_2) \tag{30}$$

and

$$\theta_i = -\tan^{-1}\left\{\frac{4Hf_p}{V_2} \sin\frac{\omega_i}{4f_p} \Big/ \cos\frac{\omega_i}{4f_p}\right\} + \phi_i \tag{31}$$

with $\phi_i$ being random phase angles as before. It is to be noted that Eq. 29 is now a function of t and $f_p$. Since $f_p$ is a function of x, this means that $u(H,t,f_p)$ is also a function of x.

Under the present circumstances, we can consider two components of strain within the surface layer; $\partial u/\partial x$ and $\partial u/\partial z$. Because of

the boundary condition, however, $\partial u/\partial z$ is always zero on the ground surface. On the other hand, the strain $\partial u/\partial x$ with u given in Eq. 29 is non-zero since the variability exists in the surface layer soil property. Therefore, $\partial u/\partial x$ strictly reflects the degree of the property variability and can conveniently be used as its measure. It is recognized that the surface strain thus obtained is not a rigorous solution but an approximate quasi-two-dimensional solution since Eq. 29 is derived on the basis of the shear beam assumption. We believe, however, that the approximation is reasonable and justified for the kind of analysis being pursued here.

The strain $\partial u/\partial x$ can be written as

$$\frac{\partial u}{\partial x} = \frac{\partial u}{\partial f_p} \cdot r \tag{32}$$

where

$$r = df_p/dx \tag{33}$$

$$\frac{\partial u}{\partial f_p} = \sqrt{2} \sum_{i=1}^{n} 2A_{oi} \sqrt{E_i^2 + F_i^2} \sin\{\omega_i t + \theta_i + \delta_i'\} \tag{34}$$

with

$$E_i = \{\omega_i \sin(\frac{\omega_i}{2f_p}) (\frac{2H^2}{V_2^2} - \frac{1}{8f_p^2}) - \frac{16H^2 f_p}{V_2^2} \sin^2(\frac{\omega_i}{4f_p})\}/q_i^{3/2} \tag{35}$$

$$F_i = \frac{H}{V_2} (2 \sin \frac{\omega_i}{2f_p} - \frac{\omega_i}{f_p})/q_i^{3/2} \tag{36}$$

$$\delta_i' = \tan^{-1}(E_i/F_i) \tag{37}$$

Then, it can be shown that

$$\overline{(\frac{\partial u}{\partial f_p})^2} = \sum_{i=1}^{n} 4S_o(\omega_i) \Delta\omega (E_i^2 + F_i^2) \tag{38}$$

where a super bar indicates the temporal average. Since r is not a function of time, we can easily show that the temporal root mean square of the strain becomes

$$\sqrt{\overline{(\frac{\partial u}{\partial x})^2}} = \sqrt{\overline{(\frac{\partial u}{\partial f_p})^2}} \cdot |r| \tag{39}$$

Figures 7(b) and 8(b) show spatial distributions of the temporal root mean square strain corresponding to the variation of $f_p$ as indicated in Figs. 7(a) and 8(a), respectively, assuming that $V_2$ = 600 m/sec. Then, the expectation of the temporal root mean square of the surface strain can be written as

$$E[\sqrt{\overline{(\frac{\partial u}{\partial x})^2}}] = \int_{-\infty}^{\infty} \int_{-\infty}^{\infty} \sqrt{\overline{(\frac{\partial u}{\partial x})^2}} \, g(f_p, r) \, df_p dr \tag{40}$$

where $g(f_p,r)$ is the joint density function of $f_p$ and r. The expectation of Eq. 39 is equivalent to the spatial average of the temporal root mean square of the surface strain theoretically considered over the infinite domain $-\infty < x < \infty$ where the random variation of the predominant frequency is given by the stationary Gaussian process $f_p(x)$. Hereafter, the expectation indicated in Eq. 40 will be referred to as the "root mean square surface strain" for simplicity.

Since the process is stationary and Gaussian, the joint density function $g(f_p,r)$ is given by

$$g(f_p,r) = \frac{1}{2\pi\bar{\sigma}_f\bar{\sigma}_r} \exp\{-\frac{(f_p-\mu_f)^2}{2\bar{\sigma}_f^2} - \frac{(r-\mu_r)^2}{2\bar{\sigma}_r^2}\} \tag{41}$$

where $\mu_f$ and $\bar{\sigma}_f$ are as defined in Eqs. 22 and 23, and

$$\mu_r = E[df_p/dx] = 0 \tag{42}$$

$$\bar{\sigma}_r^2 = Var[df_p/dx] = 6\bar{\sigma}_f^2/L^2 \tag{43}$$

The last equation is obtained by making use of the following well known relationship;

$$\bar{\sigma}_r^2\phi_r(\xi) = -\bar{\sigma}_f^2 d^2\phi(\xi)/d\xi^2 \tag{44}$$

in which $\phi_r(\xi)$ is the normalized autocovariance of $df_p/dx$.

Substituting Eqs. 39 and 41 into Eq. 40 and carrying out the integration with respect to r, we obtain

$$E[\sqrt{(\frac{\partial u}{\partial x})^2}] = \frac{\sqrt{6}}{\pi L}\int_{-\infty}^{\infty}\sqrt{(\frac{\partial u}{\partial f_p})^2}\exp\{-\frac{(f_p-\mu_f)^2}{2\bar{\sigma}_f^2}\}df_p \tag{45}$$

To remove the difficulty associated with the assumption that $f_p(x)$ is a Gaussian process and therefore can take zero or any negative values, we truncate the Gaussian density function at $f_p = f_{min}$. This reflects the fact that the shear velocity $V_1$ of the surface layer physically cannot be too small. Writing $V_{min}$ for the smallest shear velocity value we can expect of the surface layer,

$$f_{min} = V_{min}/(4H) \tag{46}$$

the root mean square value given in Eq. 45 is modified as

$$E[\sqrt{(\frac{\partial u}{\partial x})^2}] = \frac{\sqrt{6}}{\pi L}\int_{f_{min}}^{\infty}\sqrt{(\frac{\partial u}{\partial f_p})^2}\exp\{-\frac{(f_p-\mu_f)^2}{2\bar{\sigma}_f^2}\}df_p/[1-\Phi(\frac{f_{min}-\mu_f}{\bar{\sigma}_f})] \tag{47}$$

where $\Phi(\cdot)$ indicate the standardized Gaussian distribution function.

## 4. CORRELATION BETWEEN THE SURFACE STRAIN AND THE DAMAGE STATISTICS

In one of the recent Japanese studies[4], the ground predominant frequencies are evaluated at the nodal points of a grid of meridians and parallels (both at intervals of 1 km) covering the Tokyo metropolitan area. The evaluation is made based on the soil conditions at the nodes under the shear beam assumption, and for each area element of 1 $km^2$, the average $f^*$ and the standard deviation $\sigma_f^*$ of the predominant frequency are computed using the frequencies evaluated at its four corners.

The study then examines the (old but still valid) statistics taken on the underground water supply pipeline system which was in service at the time of the 1923 Kanto Earthquake and counts the number of pipe breaks and leakages in each area element resulting from the same earthquake. These numbers are divided by the length (in km) of the pipelines in each area to obtain the "break damage index" D or the "leakage damage index." Furthermore, the study correlates $f^*$ and $\sigma_f^*$ to D by dividing the $f^*$ and $\sigma_f^*$ space into the following four regions as shown in Table 1.

Table 1. Break Damage Index for Four Regions

| | $f^*$ | $\sigma_f^*$ | $\bar{D}$ |
|---|---|---|---|
| I | 1.5 ~ 3.5 | 0 < | 5.1 |
| II | 3.5 ~ 4.5 | 0 ~ 1.15 | 2.6 |
| III | 3.5 ~ 4.5 | 1.15 < | 13.3 |
| IV | 4.5 ~ 5.5 | 0 < | 2.8 |

The quantity $\bar{D}$ in Table 1 indicates the average value of D in each region. Table 1 shows that region III produces the worst damage statistics while region I the second worst. The damage indices associated with regions II and IV are much smaller than that with region III.

These Japanese data implicitly assume that the variation of the predominant frequency is two-dimensional, i.e., $f_p = f_p(x,y)$ with y being the axis perpendicular to the x-z plane in Fig. 1. Although it is not extremely difficult to deal with such two-dimensional random processes, as done in Ref. 5, the level of analytical sophistication and the amount of numerical effort required to do so would be rather inconsistent with the quality and quantity of pertinent field data available at this time. Therefore, in the present investigation, we deal with the case where the predominant frequency $f_p$ varies only in the x direction, i.e., $f_p = f_p(x)$ (thus producing only the strain $\partial u/\partial x$ on the ground surface) and where $f_p$ is evaluated along the x axis at equal intervals of 1 km. We then consider a one-dimensional equivalent of the Japanese study such that the predominant frequency in each interval of 1 km varies as a random process $f_p(x)$ characterized by Eqs. 22 - 25, with a value L common to all the

intervals but with a set of values of $\mu_f$ and $\overline{\sigma_f}$ unique to that interval. Under these circumstances, we consider as a first approximation that $\mu_f$ and $\sigma_f$ to be used for an interval are equal respectively to the sample mean and the sample standard deviation obtained on the basis of the predominant frequencies evaluated at both ends of that interval.

When L = 300 m and $V_{min}$ = 50 m/sec, we obtain Fig. 9 which indicates the root mean square (RMS) surface strains at various combinations of $\mu_f$ and $\sigma_f$; $\mu_f$ = .75, 1.25, 1.75,...6.75 Hz and $\overline{\sigma_f}$ = .125, .375, .625,..., 3.125 Hz. Purely for the purpose of establishing the trend, we assume that a particular combination of $f^*$ and $\sigma_f^*$ under the assumption of two-dimensional variation of $f_p$ will produce the same RMS surface strain as those obtained in Fig. 9. We then use Fig. 9 in conjunction with the Japanese data[4], particularly with those given in Fig. 10 which show the numbers of the area elements of 1 km² having indicated combinations of $f^*$ and $\sigma_f^*$ with blanks implying zero; $f^*$ = .75, 1.25, 1.75,..., 6.75 Hz and $\sigma_f^*$ = .125, .375, .625,..., 3.125 Hz. (These values are the same as for $\mu_f$ and $\overline{\sigma_f}$.) Thus, the $\mu_f(f^*) - \sigma_f(\sigma_f^*)$ plane in Fig. 9 can be divided into four regions, I, II, III, and IV as defined in Table 1.

The weighted averages of the RMS surface strains within regions I-IV are then computed with the numbers shown in Fig. 10 as weight. These averages, which will be referred to as the "regional RMS surface strains," are also shown in Fig. 9. The same computations are repeated for L = 500m, 800m, 1,000m and 2,000m resulting in five sets of four regional RMS surface strain values as indicated in Fig. 11(a) in terms of a bar graph. Figure 11(a) shows that the regional RMS surface strains are larger for smaller values of L within individual regions as expected, and that the largest value is observed in region III, the second largest in region I, the third in region IV and the smallest in region II for the same value of L. The latter result exhibits the same trend observed in the Japanese data[4] in Table 1 and Fig. 11(b) demonstrating how the break damage index depends upon the region. The trend is even more similar if we consider the following: assuming a larger value of L for region I than for other regions may be more appropriate since the soil conditions of region I are generally those of alluvium and are expected to be more homogeneous than in other regions where the loam generally combined with the river valley humic soil dominates. For example, take the RMS values associated with L = 500m for region I while the RMS values with L = 300m for other regions, and observe how closely the results compare with that of Fig. 11(b).

The observations made above appear to suggest that a significant correlation exists between the free field surface strain and the damage index.

## 5. CONCLUSION

The surface strains due to the random spatial variability of the soil property are evaluated under the quasi-two-dimensional assumptions. The strains are compared with the earthquake-induced damage statistics based on a field study on the underground water supply pipelines in Tokyo. The comparison indicates that a reasonably good correlation exists between these strains and the degree of the damage. This investigation is currently being extended so that the free field

strains are evaluated not at the free ground surface but at a usual depth for underground water supply pipelines where the strain component $\partial u/\partial z$ in addition to $\partial u/\partial x$ has to be considered.

## 6. ACKNOWLEDGMENT

This work was supported by the National Science Foundation under Grant No. ENV-76-09838 (Prime Contractor, Weidlinger Associates; Subcontractor, Columbia University). The authors are grateful to Professors K. Kubo and T. Katayama of the University of Tokyo for providing us with the valuable damage statistics and other information. They are also grateful to Messrs. P. Weidlinger, M. Baron and J. Wright of Weidlinger Associates for their suggestions and discussions throughout the investigation.

## REFERENCES

1) Shinozuka, M., "Digital Simulation of Random Processes in Engineering Mechanics with the Aid of FFT Technique," in "Stochastic Problems in Mechanics," edited by Ariaratnam, S.T. and Leipholz, H.H.E., University of Waterloo Press, 1974, pp. 277-286.

2) Newmark, N.M. and Rosenblueth, E., "Fundamentals of Earthquake Engineering," Prentice Hall, 1971, p. 291.

3) Kubo, K., "Dynamic Behavior of Underground Pipes during Earthquake," SEISAN-KENKYU, Monthly Journal of Institute of Industrial Science, University of Tokyo, Vol. 25, No. 2, February 1973 (in Japanese).

4) Kubo, K. and Katayama, T., "Survey on Underground Pipe Damages due to Earthquake," Unpublished Report, Tokyo Metropolitan Disaster Prevention Congress, Governor's Office, The Metropolitan Government of Tokyo (in Japanese).

5) Shinozuka, M. and Lenoe, E., "A Probabilistic Model for Spatial Distribution of Material Properties," J. Engineering Fracture Mechanics, Vol. 8, 1976, pp. 217-227.

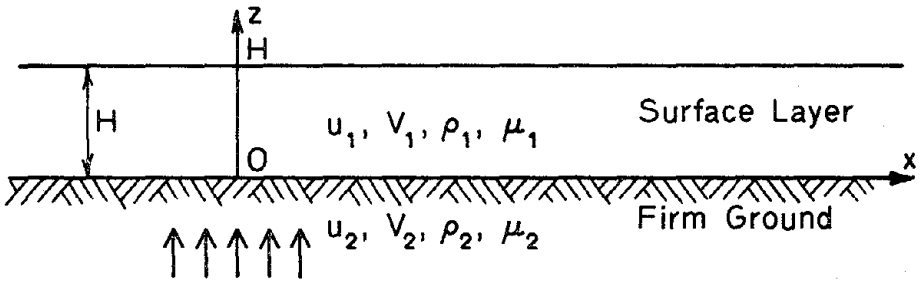


Fig. 1. Ground Model.

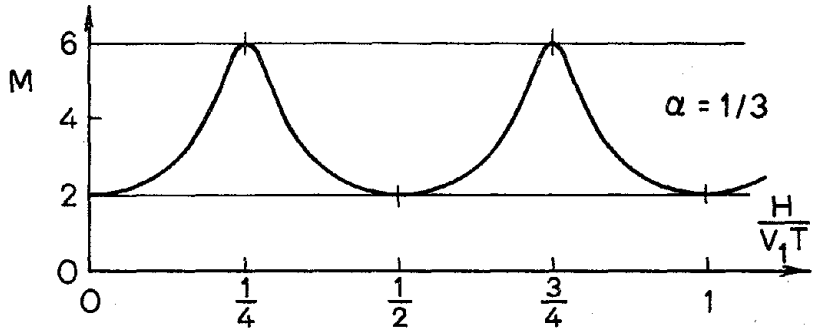


Fig. 2. Amplification Factor.

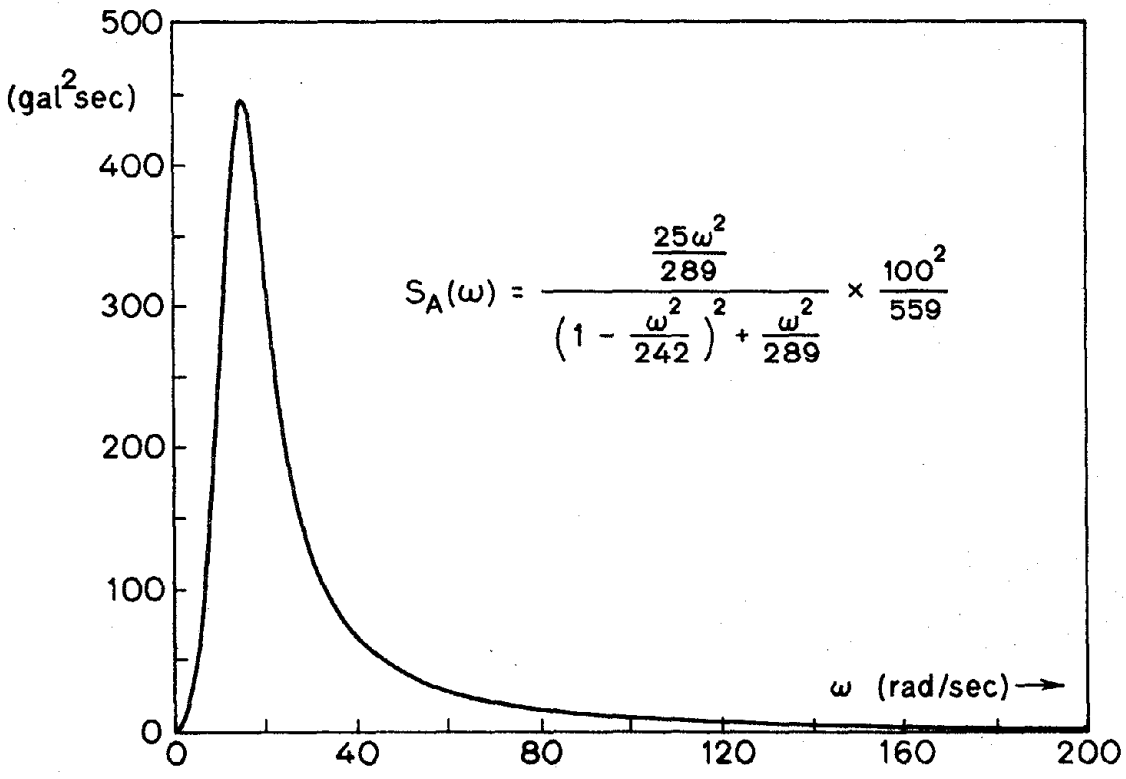


Fig. 3. Power Spectral Density (Acceleration)

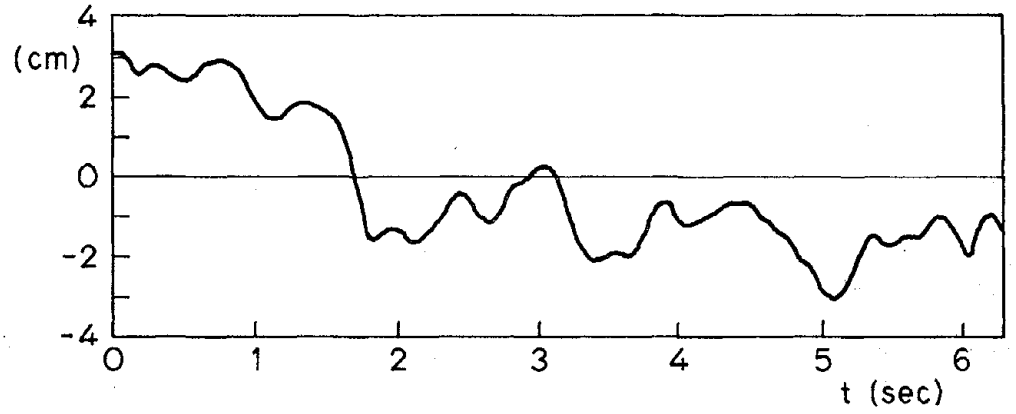


Fig. 4. Incident Wave.

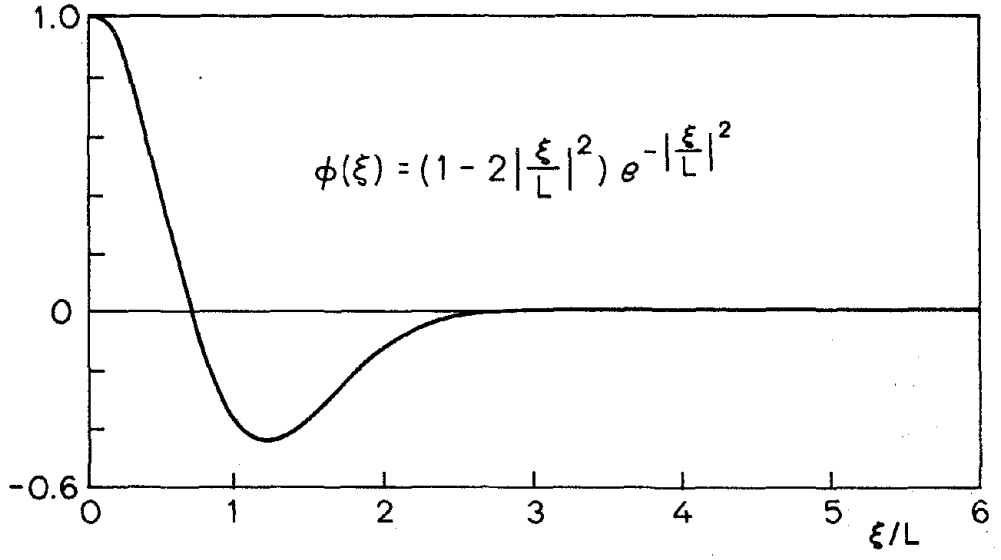


Fig.5. Spatial Auto-Covarience (normalized).

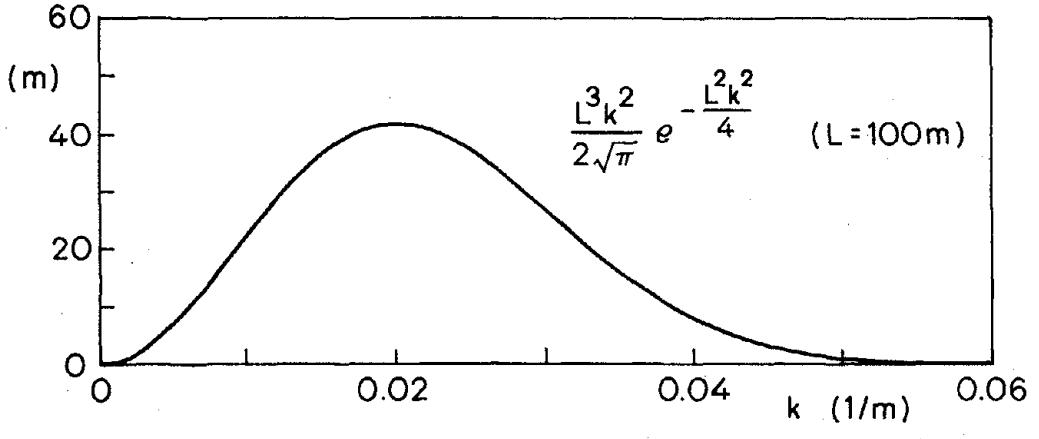


Fig. 6. Spatial Power Spectral Density.

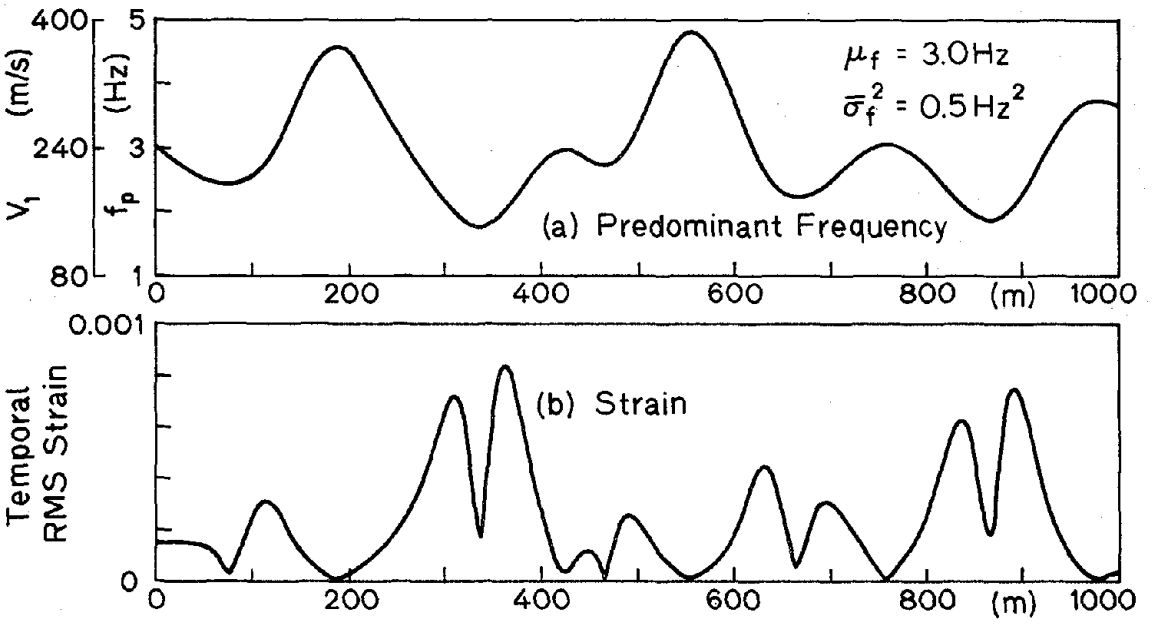


Fig. 7. Spatial Variation of Predominant Frequency and Strain (L=100m).

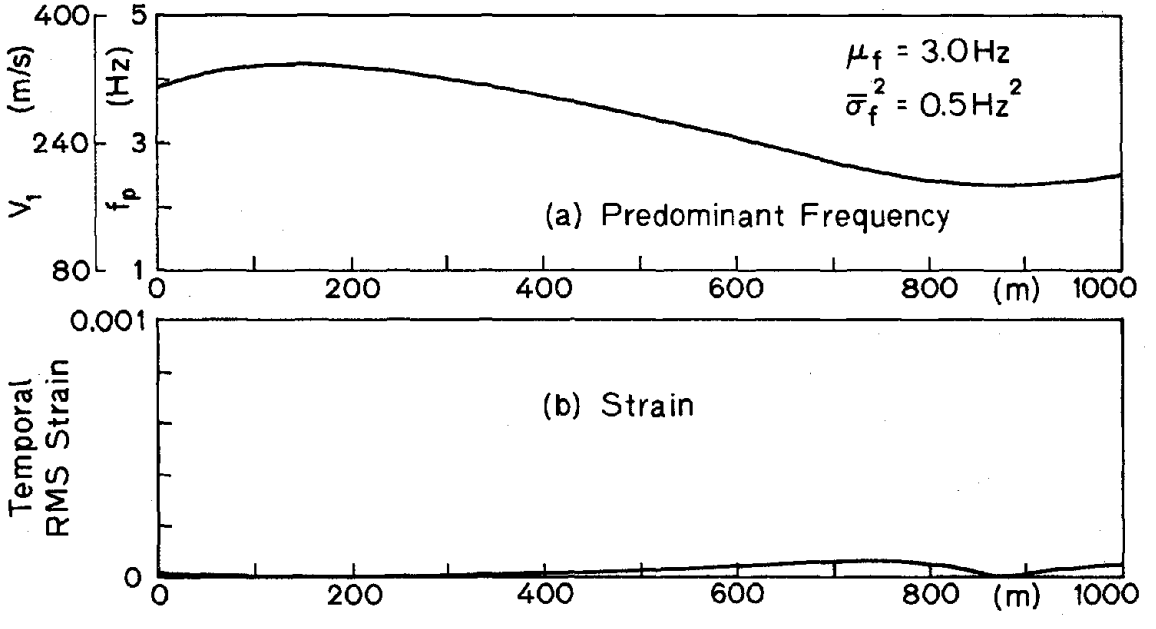


Fig. 8. Spatial Variation of Predominant Frequency and Strain (L=500m).

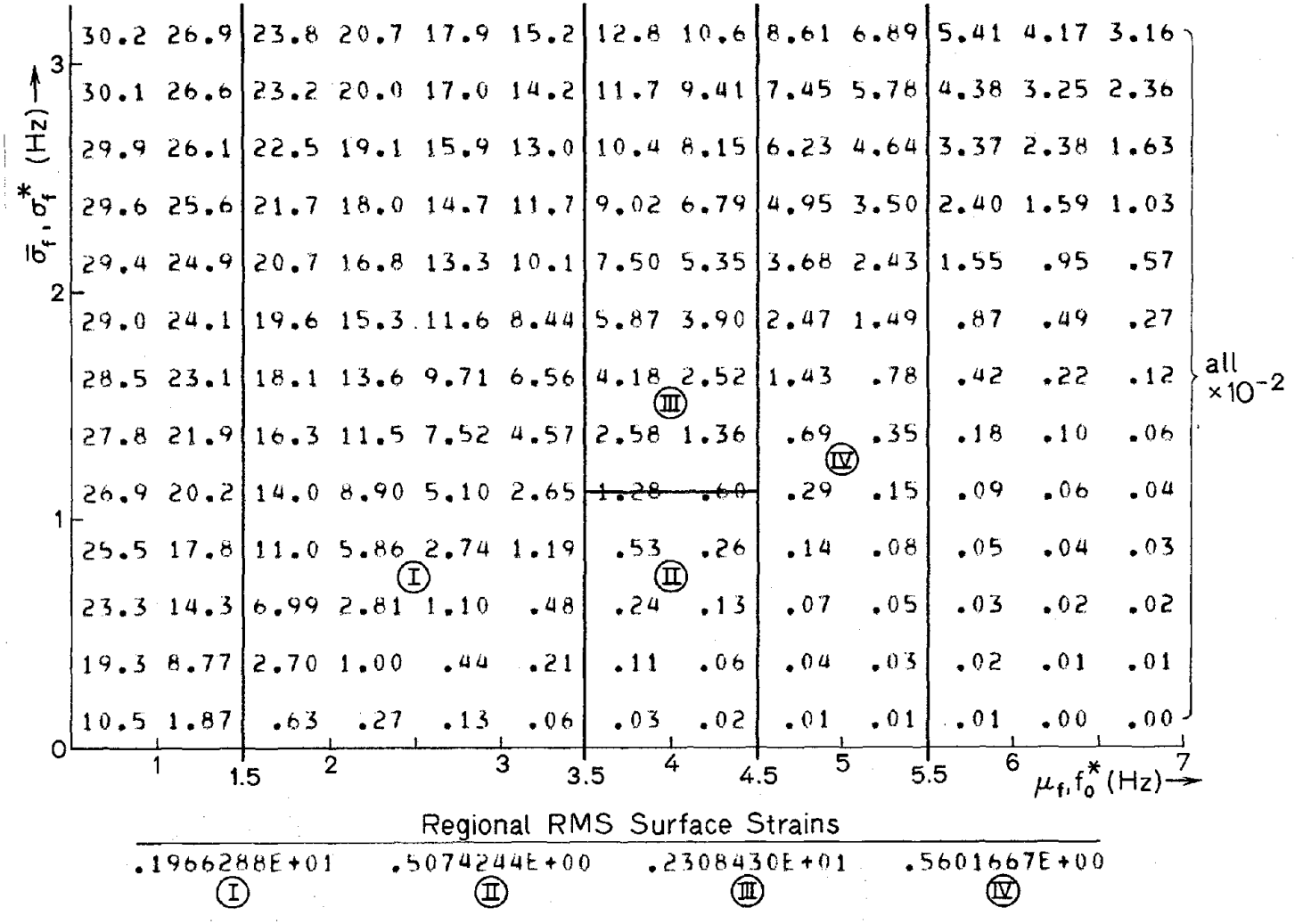


Fig. 9. RMS Surface Strain ($L = 300$ m, $V_{min} = 50$ m/s)

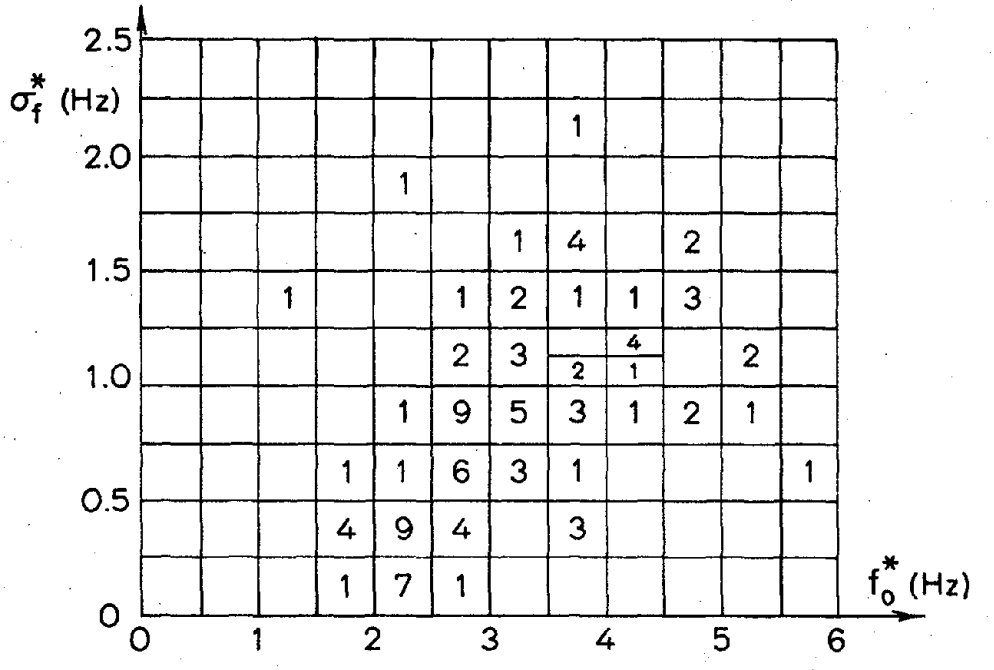


Fig. 10. Frequency Distribution of $f_0^*$-$\sigma_f^*$ Combinations

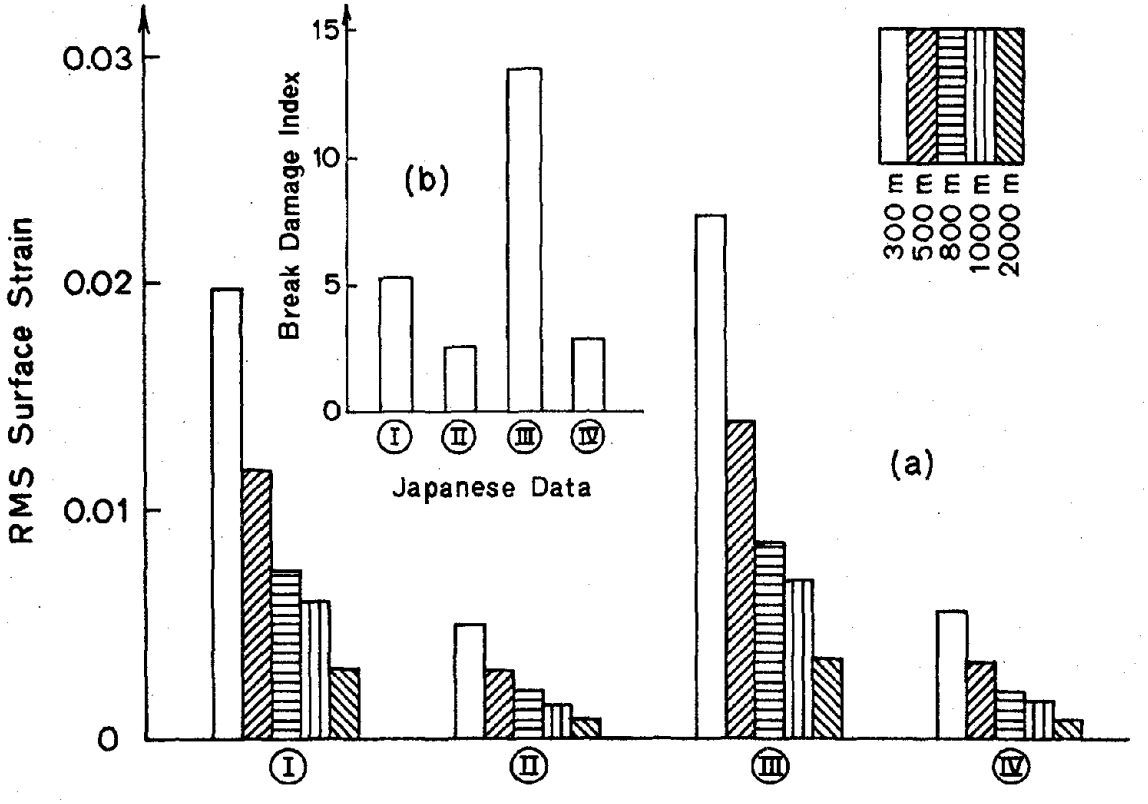


Fig. 11. Regional RMS Surface Strain.